Influence of Thermo-fluid-dynamic Parameters on Fluidics in an Expanding Thermal Plasma Deposition Chamber

G. Zuppardi and F. Romano

Abstract—Technology of thin film deposition is of interest in many engineering fields, from electronic manufacturing to corrosion protective coating. A typical deposition process, like that developed at the University of Eindhoven, considers the deposition of a thin, amorphous film of C:H or of Si:H on the substrate, using the Expanding Thermal arc Plasma technique. In this paper a computing procedure is proposed to simulate the flow field in a deposition chamber similar to that at the University of Eindhoven and a sensitivity analysis is carried out in terms of: precursor mass flow rate, electrical power, supplied to the torch and fluid-dynamic characteristics of the plasma jet, using different nozzles. To this purpose a deposition chamber similar in shape, dimensions and operating parameters to the above mentioned chamber is considered. Furthermore, a method is proposed for a very preliminary evaluation of the film thickness distribution on the substrate. The computing procedure relies on two codes working in tandem; the output from the first code is the input to the second one. The first code simulates the flow field in the torch, where Argon is ionized according to the Saha's equation, and in the nozzle. The second code simulates the flow field in the chamber. Due to high rarefaction level, this is a (commercial) Direct Simulation Monte Carlo code. Gas is a mixture of 21 chemical species and 24 chemical reactions from Argon plasma and Acetylene are implemented in both codes. The effects of the above mentioned operating parameters are evaluated and discussed by 2-D maps and profiles of some important thermo-fluid-dynamic parameters, as per Mach number, velocity and temperature. Intensity, position and extension of the shock wave are evaluated and the influence of the above mentioned test conditions on the film thickness and uniformity of distribution are also evaluated.

Keywords—Deposition chamber, Direct Simulation Mote Carlo method (DSMC), Plasma chemistry, Rarefied gas dynamics.

I. INTRODUCTION

THE thin film deposition process (or coating) on a surface, i.e. a substrate, consists in creating a solid layer from chemical reactions in the gas (or liquid) or directly from chemical reactions with the substrate material. A thin film has a thickness from few nanometers to about 100 micrometers.

G. Zuppardi is with the Department of Aerospace Engineering, University of Naples "Federico II", Piazzale Tecchio 80, 80125 Naples, Italy (corresponding author to provide phone: +39-081-7682349; fax: +39-081-7682351; e-mail: zuppardi@unina.it).

F. Romano is with the Department of Aerospace Engineering, University of Naples "Federico II", Piazzale Tecchio 80, 80125 Naples, Italy; e-mail: francesco.romano@unina.it)..

Due to their excellent material properties (hardness, adhesion, chemical stability), the thin films are of great interest in the field of electronic manufacturing such as: magnetic recording media, semiconductors, Liquid Crystal Displays (LCD), solar cells, corrosion protective coating and so on.

The deposition techniques basically fall into two wide categories, depending on whether the deposition process is chemical (Chemical Vapor Deposition: CVD) or physical (Physical Vapor Deposition: PVD). In the CVD process, a fluid precursor undergoes a chemical change at the substrate, forming a solid layer. In the PVD process, the deposition is obtained by the condensation of vaporized material on the substrate.

Different types of deposition processes have been developed. In the present paper the Expanding Thermal Plasma (ETP) technique, developed by van de Sanden and co-workers at the University of Eindhoven [1], [2], is considered. In this deposition process, Argon is ionized in a torch in order to transform it into a plasma and therefore into a chemically reactive species. A precursor like Acetylene (C_2H_2) or Methane (CH_4) or Silane (SiH_4) is then injected into the plasma jet. Thanks to the high reactivity level of Argon ion, the chemical composition of the gas mixture changes, generating a lot of different species. All species flow toward a substrate and some of them deposit on it, forming a film.

It is clear that fluidics play an important role in the deposition process. For this reason the flow field in a deposition chamber has been already studied and simulated by several codes, based on different approaches: Computational Fluid-Dynamics (CFD) [3], Molecular Dynamics (MD) [4], Direct Simulation Monte Carlo (DSMC) [5] and also by hybrid CFD-DSMC procedures [6], [7].

In this paper, a computing system, for simulating the flow field in a deposition apparatus, is proposed. The procedure is made of two codes working in tandem; the output from the first one is the input to the second one. The first code simulates the flow field in the torch and in the first part of the nozzle; this code can be considered like a pre-processor. The second one is a commercial DSMC code (DS2V [8]), simulating the flow field in the remainder of the nozzle and in the whole chamber; the present computing system can be considered as partially hybrid.

World Academy of Science, Engineering and Technology
International Journal of Aerospace and Mechanical Engineering
Vol:4, No:11, 2010

As shown later and as already verified by other researchers [5], at the usual test conditions, the flow field in a deposition chamber is rarefied enough for a proper simulation by a DSMC code. Furthermore, as the deposition process consists in the stick or aggregation of an atom at a time, impinging onto the substrate, using the molecular approach or the DSMC method looks to be particularly suitable for evaluating some characteristics of the film. Preliminary tests, considering only inert Argon, have been already carried out by the present authors [9], in order to state general operative conditions both for the pre-processor and for DS2V such as: geometrical configuration of the computing dominion, some computing parameters typical of the DSMC codes, a method for a preliminary evaluation of the uniformity of film and so on.

The ultimate purpose of this work is to make a sensitivity analysis of the operating parameters of a ETP deposition chamber and therefore to provide an operator, or even a designer, with a further computing tool, supporting the choice of optimal test parameters in the working of a ETP deposition chamber. More specifically, the flow field in a deposition chamber similar in shape, dimensions and operating parameters to that in Eindhoven, is simulated in order to verify the influence of: electrical power, supplied to the torch, mass flow rate of C_2H_2 and different thermo-fluid-dynamic conditions due to different supersonic, conical nozzles, i.e. with different area ratio (exit area/throat area) and length. The present simulation is related to a mixture of Ar, Ar^+ and C_2H_2 and related products of chemical reactions, for the production of hydrogenated amorphous carbon (a-C:H) film.

This sensitivity analysis was proper because all these parameters affect the flow field in a deposition chamber and, more specifically, the intensity, position and extension of the shock wave and eventually the uniformity of film distribution on the substrate. The computations quantified also the effects of the Argon ionization degree and its influence on the occurrence of chemical reactions and therefore on the gas chemical composition. More specifically, the influence on the molar fraction of the chemical species forming the film has been also evaluated.

II. ETP DEPOSITION APPARATUS AND PLASMA CHEMISTRY

A typical ETP deposition apparatus (Fig.1) is made up of a torch, a nozzle, an expansion cylindrical chamber (or reactor) and a substrate holder. The chamber inlet section is the same like the nozzle exit section. A pump holds pressure in the chamber at low values; between 10 and 100 N/m^2.
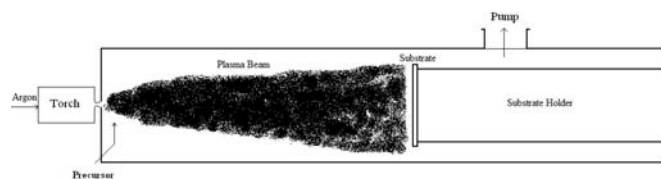

Fig. 1 Typical deposition apparatus

TABLE I
CHEMICAL SPECIES AND REACTIONS

N	Chemical Reactions	K (m^3/s)	Reaction yields	ΔH_f (eV)
1	$Ar^+ + C_2H_2 \rightarrow Ar + C_2H_2^+$	4.2×10^{-16}	1	0
2	$C_2H_2^+ + e \rightarrow C_2H + H$	9.5×10^{-14}	0.5	0
3	$C_2H_2^+ + e \rightarrow C_2 + H + H$	9.5×10^{-14}	0.3	0
4	$C_2H_2^+ + e \rightarrow CH + CH$	9.5×10^{-14}	0.13	0
5	$C_2H_2^+ + e \rightarrow CH_2 + C$	9.5×10^{-14}	0.05	0
6	$C_2H_2^+ + e \rightarrow C_2 + H_2$	9.5×10^{-14}	0.02	0
7	$Ar^+ + C_2H \rightarrow Ar + C_2H^+$	4.2×10^{-16}	1	0
8	$C_2H^+ + e \rightarrow C_2 + H$	7.2×10^{-14}	0.47	0
9	$C_2H^+ + e \rightarrow C + CH$	7.2×10^{-14}	0.38	0
10	$C_2H^+ + e \rightarrow C + C + H$	7.2×10^{-14}	0.15	0
11	$Ar^+ + C_2 \rightarrow Ar + C_2^+$	4.2×10^{-16}	1	0
12	$C_2^+ + e \rightarrow C + C$	6.0×10^{-14}	1	0
13	$Ar^+ + CH \rightarrow Ar + CH^+$	4.2×10^{-16}	1	0
14	$CH^+ + e \rightarrow C + H$	4.5×10^{-14}	1	0
15	$Ar^+ + CH_2 \rightarrow CH_2^+ + Ar$	4.2×10^{-16}	1	0
16	$CH_2^+ + e \rightarrow CH + H$	5.2×10^{-14}	0.25	0
17	$CH_2^+ + e \rightarrow C + H_2$	5.2×10^{-14}	0.12	0
18	$CH_2^+ + e \rightarrow C + H + H$	5.2×10^{-14}	0.63	0
19	$C + C_2H_2 \rightarrow C_3 + H_2$	2.7×10^{-16}	1	1.28
20	$CH + C_2H_2 \rightarrow C_3H + H_2$	2.0×10^{-16}	1	1.91
21	$CH_2 + C_2H_2 \rightarrow C_3H_3 + H$	3.0×10^{-16}	1	0.56
22	$C_2 + C_2H_2 \rightarrow C_4H + H$	2.7×10^{-16}	0.5	0.42
23	$C_2 + C_2H_2 \rightarrow C_4 + H_2$	2.7×10^{-16}	0.5	0.97
24	$C_2H + C_2H_2 \rightarrow C_4H_2 + H$	1.3×10^{-16}	1	0.22

The ETP technique consists in generating thermal plasma of argon. Precursor gas (S_iH_4 or C_2H_2 or CH_4) can be injected into the plasma stream either by an injection ring, placed in the chamber near the inlet section, or in the nozzle, or directly into the background [1], [4]. Precursor reacts with electrons and ions in the plasma, producing radical, reactive species. The plasma mixture expands supersonically into the reactor and then is compressed by a shock wave. Plasma flows toward the substrate where deposition occurs, forming a film.

The chemical reactions involved in an ETP deposition chamber, using as precursor C_2H_2, have been already considered by a number of researchers such as Mankelevich [10], Ariskin [11], Benedikt [12], [13]. In the present paper the chemical reactions reported by Benedikt [12] have been used. In the present paper, 21 chemical species (Ar, Ar^+, C_2H_2, $C_2H_2^+$, C_2H, H, C_2, CH, C_2H^+, C, C_2^+, CH^+, CH_2, CH_2^+, H_2, C_3, C_3H, C_3H_3, C_4H, C_4, C_4H_2) have been taken into account. These species react according to 24 forward, plasma chemistry reactions, taken by Benedikt [12], and reported in Table I together with the reaction rates (K (m^3/s)), reaction yields and heats of formation (ΔH_f (eV)). The reactions are: 5 charge transfer, 13 dissociative recombination, 6 exothermic, radical neutral reactions and have been implemented both in the pre-processor and in the DSMC code. As reported by Benedikt [12], the film is produced by the deposition of carbon (C and C_2) and also partially of two species based on carbon (CH and C_2H).

The deposition process depends on the sticking factor, defined as the ratio of the number of stuck molecules on the number of impinged molecules. An important parameter in the plasma chemistry of Ar^+ and C_2H_2 is played by the ratio of the molecular flux of C_2H_2 (Φ_{C2H2}) on the molecular flux of Ar^+ (Φ_{Ar+}): $F = \Phi_{C2H2}/\Phi_{Ar+}$. In fact, according to Benedikt [12],

World Academy of Science, Engineering and Technology
International Journal of Aerospace and Mechanical Engineering
Vol:4, No:11, 2010

[13], the preeminent reactions are: the charge transfer and dissociative-recombination reactions when F<1, the radical-neutral reactions when F>1.

III. DSMC Method and DS2V code

It is well known that the DSMC method [14], [15] is nowadays the only available method to solve a rarefied flow field, overcoming the failure, in this regime, of the phenomenological equations of Newton, Fourier, and Fick and therefore of the Navier–Stokes equations. This method relies on the kinetic theory of gases and simulates the evolution of millions of simulated molecules: each simulated molecule represents a large number of real molecules in the physical space.

Movement and evolution of each molecule is produced by collisions with other molecules and with the body under study, in both cases exchanging momentum and energy. Excitation of rotational and vibrational degrees of freedom and chemical reactions can be also taken into account. The computational domain, including the test body, is divided in cells; these are used only for selecting the colliding molecules and for sampling the macroscopic properties. Displacement of each molecule from a cell to another one is the product of the velocity (that is the resultant of the convective and thermal velocities) and a time step. Macroscopic thermo-fluid-dynamic quantities of the flow field (density, temperature, pressure and so on) are computed in each cell as an average over the molecules.

The DSMC code, used in the present application, is DS2V (Ver.4.5) [8]. DS2V simulates 2-D plane/axial-symmetric flow fields. The most important features of the code, making it particularly suitable for the present application, are: i) it can consider chemical reactions involving electrons and ions; gas is assumed to be electrically neutral, being the number of electrons equal to the number of cations. Electrons move with their computationally linked ions, ii) each chemical species impinging onto a surface can interact with a surface, according to the Maxwell interaction models: specular and/or diffusive, fully accommodate. Even though DS2V can consider wall reactions (as per dissociation, recombination and transfer), in the present applications, these reactions were not simulated.

DS2V is widely tested and worldwide accepted; it is "sophisticated" and advanced (a sophisticated DSMC code is called also DSMC07). The procedures, making a DSMC code sophisticated [16], [17] therefore superior with respect to a "basic" DSMC code (a basic DSMC code is called also DSMC94) are: i) it relies on two sets of cells (collision and sampling cells) with the related cell adaptation, ii) it implements methods promoting nearest neighbor collisions, iii) the same collision pair can not have sequential collisions, iv) it generates automatically computational parameters such as numbers of cells and of simulated molecules by the input number of megabytes, v) it uses a radial weighting factor in solving axial-symmetric flow fields, vi) it provides optimal time step. DS2V is advanced because allows the user to check

on line, during the run, the adequacy of the number of simulated molecules and therefore the quality of the results by means of the display of the maximum and averaged values of the ratio of the mean collision separation (mcs) to the local mean free path (λ). Bird [8] suggests 0.2 as a limit value of mcs/λ for an optimal quality of the run. Moreover, DS2V provides facilities very useful for the user for checking on line the evolution of the run and therefore for evaluating the reliability of the results.

IV. Rarefaction parameters

The rarefaction analysis relies on two local rarefaction parameters: local Knudsen number Kn_G and parameter P of Bird [14]. Kn_G is defined as the ratio of the local mean free path (λ) and the scale factor (L_G) of the gradient of a generic macroscopic quantity G: temperature (T), pressure (p), density (ρ) and velocity (V):

$$L_G = \frac{G}{(dG/ds)} \qquad (1)$$

s is an abscissa in the flow direction. According to Bird [14], the classification of rarefaction, in terms of Kn_G, is:

$Kn_G < 0.1$ Continuum with validity of the Navier-Stokes equations,

$0.1 < Kn_G < 0.2$ Continuum without validity of the Navier-Stokes equations; this regime is called also continuum low density regime,

$Kn_G > 0.2$ Non continuum; a molecular approach is necessary.

Parameter P of Bird [14] reads:

$$P = \frac{\sqrt{\pi}}{2} S \frac{\lambda}{\rho} \left| \frac{d\rho}{ds} \right| \qquad (2)$$

where S is the speed ratio, defined as the ratio of velocity and the most probable thermal velocity (c):

$$S = \frac{V}{c} \qquad (3)$$

$$c = \sqrt{\frac{2k_B T}{m}} \qquad (4)$$

k_B is the Boltzmann constant and m is the mass of a molecule. Parameter P is used to check if a flow field overcomes the "continuum breakdown" limit. According to Bird, this limit starts from P=0.02.

V. Computing procedure

As said before, the computing procedure relies basically on two codes: pre-processor and DS2V, working in tandem; the output from the pre-processor is the input to DS2V. A third code, or post-processor, computes the above mentioned rarefaction parameters from the DS2V output.

A. Pre-processor

This code is based on the hypothesis of steady, inviscid, thermally non conductive, quasi-one-dimensional flow. Each gas in the mixture is considered to be thermally perfect. The code simulates the flow field in the torch and in first part of the divergent part of the supersonic nozzle up to 90% of its

World Academy of Science, Engineering and Technology
International Journal of Aerospace and Mechanical Engineering
Vol:4, No:11, 2010

length (L), including a thin part after the injection of precursor. The thermo-fluid-dynamic parameters (temperature, velocity, number density) and composition of the mixture in terms of molar fraction (α) of each species (α_{Ar}, α_{Ar+}, α_{C2H2}, α_{C2H2+}, α_{C2H},…) are input to DS2V (Fig. 2).

The pre-processor does not model the flow field in the convergent part of the nozzle. It computes the thermo-fluid-dynamic parameters in the throat by the conservation of the mass flow rate and by imposing the Mach number (Ma) equal to one at the nozzle throat. These are the starting conditions for the solution of the flow field in the divergent part. The molar fractions of Ar and Ar^+ do not change in the nozzle.
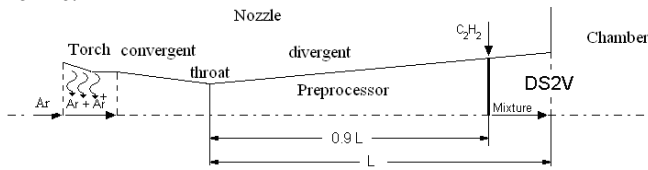

Fig. 2 Schematic of the torch and of the nozzle

The system of equations on which pre-processor relies is:

$$\rho VA = \cos t. \tag{5.a}$$

$$p + \rho V^2 = \cos t. \tag{5.b}$$

$$h + V^2/2 = \cos t. \tag{5.c}$$

where: A is the conduct area and h is the thermodynamic enthalpy. Relying on validity of the Dalton law and considering Argon as reference gas, pressure and thermodynamic enthalpy read:

$$p = R_{Ar}T\rho\left(\beta_{Ar} + \beta_{C_2H_2}\frac{m_{Ar}}{m_{C_2H_2}} + \beta_{C_2H}\frac{m_{Ar}}{m_{C_2H}} + \right.$$
$$\left. + ... + \beta_{C_4H_2}\frac{m_{Ar}}{m_{C_4H_2}}\right) \tag{6.a}$$

$$h = \frac{R_{Ar}T}{2}\left((n_{Ar}+2)\beta_{Ar} + \right.$$
$$+ (n_{C_2H_2}+2)\beta_{C_2H_2}\frac{m_{Ar}}{m_{C_2H_2}} + (n_{C_2H}+2)\beta_{C_2H}\frac{m_{Ar}}{m_{C_2H}} +$$
$$\left. + ... + (n_{C_4H_2}+2)\beta_{C_4H_2}\frac{m_{Ar}}{m_{C_4H_2}}\right) \tag{6.b}$$

where R_{Ar} is the constant of Argon, n is the number of freedom degrees of the molecules and β is the mass fraction of each chemical species in the mixture, computed by the chemical reactions in Table I. The energy released by the exothermic reactions 19 thru 24 and the variability of n with temperature are also taken into account.

In the present computations, the torch (Perkin-Emler, 9MB-M), installed in the plasma wind tunnel "Small Planetary Entry Simulator" (SPES) at the University of Naples "Federico II", is simulated. The conduct of this torch is made of a convergent nozzle (diameter of the inlet section 0.013 m, length 0.009 m) and a constant area conduct (diameter 0.008 m, length 0.023 m). In the present simulations: Argon is supposed to be injected into the torch at ambient temperature (300 K) and with an injection velocity of 100 m/s. Furthermore, electrical power is considered to be distributed uniformly along the torch conduct. Successful processing of tests in SPES [18], [19] verified that these assumptions are proper.

First ionization of Argon, quantified by the molar faction of Argon cations α_{Ar+}, is computed by the Saha's equation [20]:

$$\log_{10}\left(\frac{\alpha_{Ar+}^2}{1-\alpha_{Ar+}^2}p\right) = \frac{-5050E_{ion}}{T} + 2.5\log_{10}(T) - 6.5 \tag{7}$$

where pressure is in atm. and E_{ion} is the first ionization energy in eV.

Simulations have been carried out considering three possible supersonic, convergent-divergent conical nozzles installed in SPES, here labelled A, B, C. The inlet section diameter of all nozzles is the same (0.022 m), the length of the convergent part is 0.046 m for nozzles A and B and 0.025 m for nozzle C. The geometrical characteristics of the divergent parts are:

Nozzle A: throat diameter 0.011 m, exit section diameter 0.022 m (area ratio 4), length 0.061 m,
Nozzle B: throat diameter 0.011 m, exit section diameter 0.05 m (area ratio 20), length 0.1553 m,
Nozzle C: throat diameter 0.008 m, exit section diameter 0.06 m (area ratio 56), length 0.198 m.

B. DS2V

Fig. 3 shows a schematic of the deposition chamber reported in Fig. 1. In order to consider plausible tests, dimensions of the simulated chamber are the same like the ones of the chamber at the University of Eindowen (length 0.8 m, diameter 0.16 m) as well as the dimensions of the substrate holder (length 0.35 m, diameter 0.1 m) and of the slot (length 0.02 m) linking the chamber with a pump. In the present simulation, the exit section is simulated by an annulus around the chamber, the exit velocity (V_E), input to DS2V, is computed by the balance equation of the mass flow rate.
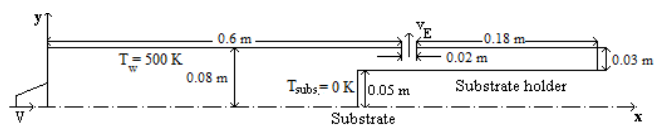

Fig. 3 Schematic of the deposition chamber

World Academy of Science, Engineering and Technology
International Journal of Aerospace and Mechanical Engineering
Vol:4, No:11, 2010

The surface temperature of the chamber and of the substrate holder is 500 K. Molecule-surface interaction model is fully accommodate for all molecules impinged onto the surfaces of the chamber and of the substrate holder. Usually in space applications, when the rarefaction level of a flow field around a body is not extremely high such as in the present cases (as shown later), the hypotheses of a diffusive, fully accommodate model holds. The deposition process on the substrate is simulated by considering: i) fully accommodate gas surface interaction model for the species forming the film (C, C_2, CH and C_2H); for the interaction of these species, the substrate temperature is put at zero, ii) a specular interaction model for other species. The hypothesis of zero temperature is a numerical artifice for a correct simulation of the sticking process. In fact, the velocity of the molecules re-emitted by the diffusive model is, in turn, zero. Consequently, the molecules do not move from the surface and do not return to the flow, completing in this way, the simulation of the sticking process. By this procedure, in the present application, a value of the sticking factor equal to one is simulated. The profile of the molecule number flux (N_f ($m^{-2}s^{-1}$)) to the substrate, output by DS2V, provides a very preliminary measure of the film thickness and of its uniformity.

For all computations, the input number of megabytes was 150, providing a proper number both of cells and of simulated molecules. The numbers of simulated molecules was about 1.5×10^7; this number was proper because the condition of mcs/λ<0.2 was always met; the maximum value, over all runs was 0.19. Furthermore, the simulation time was long enough to satisfy the condition of stationary state; the ratio of simulated time to reference time was between 6 and 10. The reference time is the time necessary to cross the computing domain, in this case the length of the chamber, at velocity equal to the one at the inlet section.

C. Post- processor

A post-processor code has been developed for the rarefaction analysis of the flow field in the chamber; the output from DS2V is the input to the post-processor. The rarefaction analysis focuses on parameter P by Bird and on Kn_V and Kn_T, all computed along the chamber axis x (Fig. 3) therefore, dG/ds≅dG/dx. Derivatives have been approximated numerically at each position x_i, by: $(dG/dx)_i \cong (G_{i+1} - G_i)/(x_{i+1} - x_i)$. The mean free path, at each point i, is provided in output by DS2V.

VI. ANALYSIS OF THE RESULTS

Analysis relies on 11 computer tests and considers the effects of: i) thermo-fluid-dynamic parameters linked to the nozzles A, B and C, ii) electrical power (P), in the interval from 1 to 13 kW and iii) precursor mass flow rate ($\dot{m}_{C_2H_2}$), in the interval from 1 to 15 sccs (sccs is for standard cubic centimeter per second; 1 sccs=2.69×10^{19} particles/s).

The typical mass flow rate of Argon, used in the tests in the deposition apparatus in Eindhoven, is 100 sccs (1.787×10^{-4} kg/s) [12]; this value has been kept also in all present runs.

A.. Torch and nozzle

The influence of the electrical power in the torch is shown in Fig. 4 where the profiles of molar faction of Argon cations α_{Ar+} (or ionization degree) are reported along the torch axis; α_{Ar+} ranges from 0.02, at the end of the torch when P=1 kW, to a complete ionization, even at beginning of the torch conduct, when P=11 and P=13 kW.
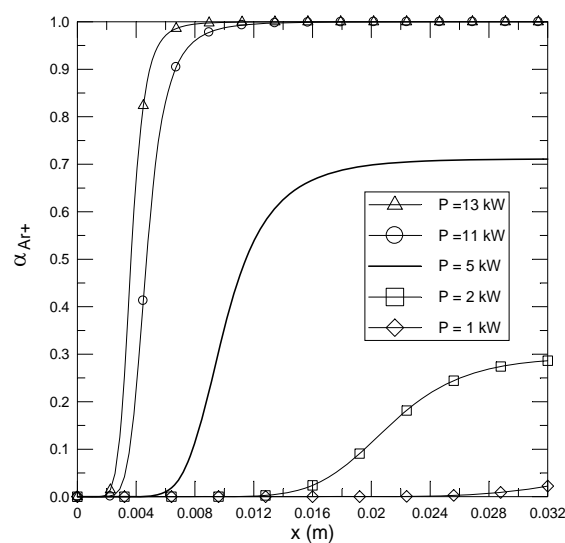

Fig. 4 Profiles of Argon ionization degree along the torch axis

Table II reports the fluid-dynamic parameters and the molar fractions of the most meaningful components of the mixture (α_{Ar+}, α_{C2H2}), computed by the pre-processor at 90% of the length of the divergent part of each nozzle and, as said before, input to DS2V. Each test is identified by a letter and by two numbers; the letter indicates the nozzle, the first number indicates the power in kW and the second number indicates the precursor mass flow rate in sccs. As the geometrical characteristics of nozzle A are comparable with those of the nozzle in the deposition apparatus in Eindhoven and the typical electrical power and mass flow rate of C_2H_2, used in that apparatus, are 5 kW and 5 sccs [6], test A-5-5 can be considered as the most representative, thus the related results have to be considered as reference data.

As chemical processes (Table I) are closely linked to the Argon ionization degree, the mixture composition, input to DS2V, changes strongly with power. Fig. 5 reports, as typical example, the profiles of the molar fraction of five chemical species (C, C_2, H, $C_2H_2^+$ and Ar^+), chosen randomly, as functions of power. Tests ran using nozzle A and a mass flow rate of precursor of 5 sccs. The molar fractions grew of 1 or even 2 orders of magnitude in the power interval 1-13 kW.

World Academy of Science, Engineering and Technology
International Journal of Aerospace and Mechanical Engineering
Vol:4, No:11, 2010

B. Rarefaction

Post-run rarefaction analysis verifies that using the DSMC approach is proper. Fig. 6 reports the profiles, along the chamber axis, of P (a), Kn_T (b) and Kn_V (c) for test A-5-5. All parameters agree in stating a pretty high rarefaction level in the

TABLE II
INPUT PARAMETERS TO DS2V CODE

Test	V [m/s]	T [K]	N [1/m³]	V_E[m/s]	α_{Ar+}	α_{C2H2}
A-13-5	4737	12543	2.24×10^{21}	149	0.521	0.479
A-11-5	4118	9386	2.52×10^{21}	130	0.575	0.425
A-5-5	2772	4327	3.56×10^{21}	87	0.497	0.301
A-2-5	2587	3794	3.79×10^{21}	81	0.205	0.283
A-1-5	2287	3006	4.23×10^{21}	72	0.017	0.253
A-5-15	2050	2359	5.70×10^{21}	65	0.310	0.564
A-5-10	2346	3025	4.63×10^{21}	74	0.382	0.463
A-5-2	3131	5946	2.92×10^{21}	99	0.606	0.147
A-5-1	3276	6820	2.70×10^{21}	103	0.654	0.079
B-5-5	1714	1212	1.46×10^{21}	257	0.188	0.735
C-5-5	1380	902	1.30×10^{21}	300	0.126	0.823

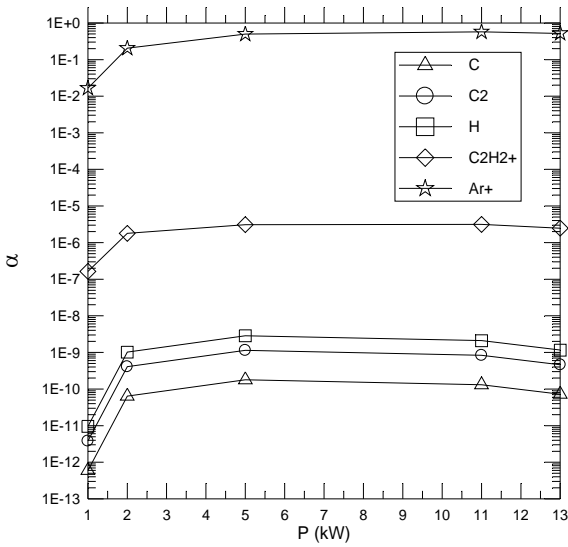Fig. 5 Profiles of molar fraction of some chemical species input to DS2V for nozzle A and $\dot{m}_{C2H2}$=5 sccs

chamber, even by the overcoming of the "continuum break down" limit, making necessary a molecular approach to solve the flow field in the chamber. The same remark holds also for other tests. In fact, the value of P, averaged along the chamber axis, ranges from 0.10 to 0.22 in the mass flow rate interval, and from 4.5×10^{-2} to 0.26 in the power interval. Parameter P got the average values 5.5×10^{-2} and 4.6×10^{-2} for tests B-5-5 and C-5-5, respectively. For test with low mass flow rate, as per test A-5-1, P, Kn_T and Kn_V got values in some points along the chamber axis also of the order of 10^{-3}, identifying some cells in which the flow field is continuum. However the feature of sophisticated code allowed DS2V to be used also in these severe conditions, not allowable to a "basic" DSMC code.
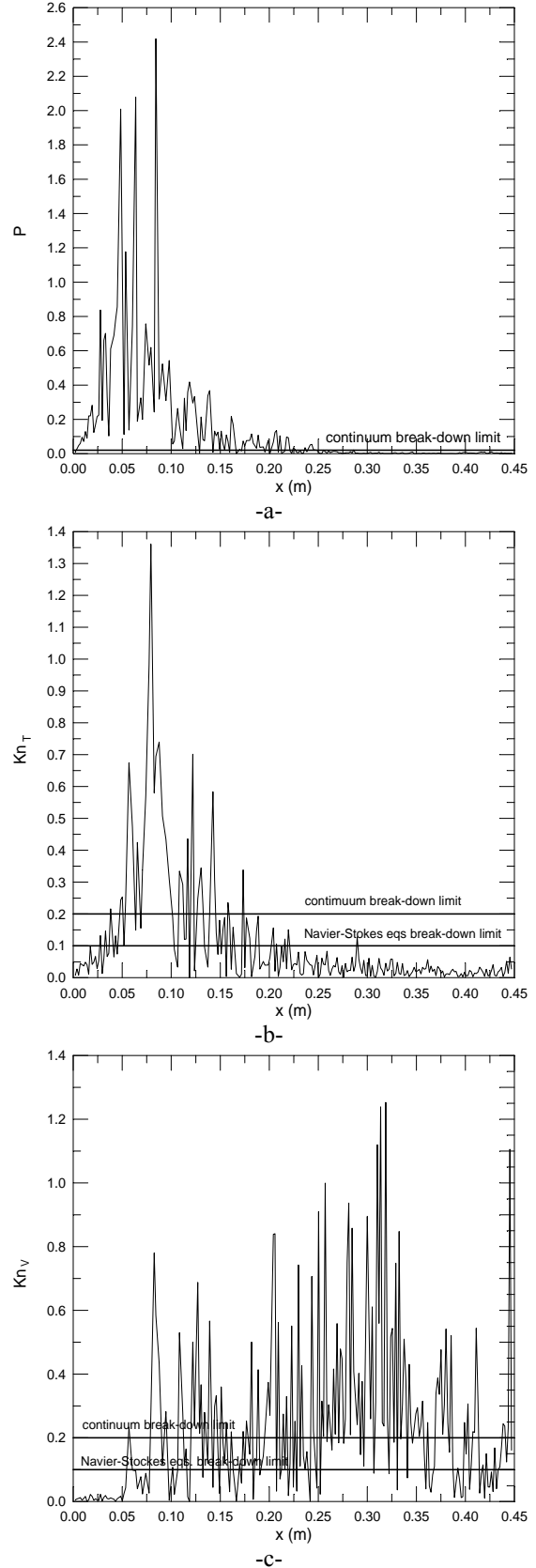

-a-

-b-

-c-

Fig. 6 Profiles of parameter P (a), Kn_T (b) and Kn_V (c) along the chamber axis: test A-5-5

World Academy of Science, Engineering and Technology
International Journal of Aerospace and Mechanical Engineering
Vol:4, No:11, 2010

C. Fluidics

The Mach number is one of the most meaningful fluid-dynamic parameters. In fact, it provides information about intensity, extension and shape of the shock wave. Fig. 7 shows the two dimensional (2-D) map of the Mach number for test A-5-5. This map verifies that the expansion, produced by the nozzle, continues in the chamber and is stopped by a shock wave. The shock wave has the typical "leaf–blade" shape. The position of the shock wave is defined as the abscissa (x_s (m)) where the Mach number attains a relative maximum and its extension or thickness (Δx_s (m)) is defined as the region included between x_s and the point where the Mach number goes back to be again less than one.
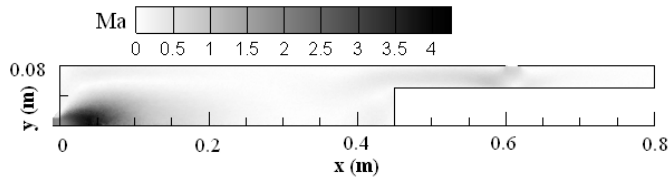

Fig. 7 2-D map of Mach number in the chamber for test A-5-5

The influence of the different test conditions, on the Mach number profile along the chamber axis, therefore on the shock wave, is shown in Fig. 8. Table III reports, for all tests, the values of some meaningful parameters such as: i) Mach number at the chamber inlet section (Ma_i), ii) maximum value of the Mach number (Ma_{max}) in the chamber (this is a measure of intensity of the shock wave), iii) position and iv) extension of the shock wave.

TABLE III
SHOCK WAVE PARAMETERS IN THE CHAMBER

Test	Ma_i	Ma_{max}	x_s (m)	Δx_s (m)
A-13-5	2.03	3.25	0.03	0.11
A-11-5	2.02	3.27	0.03	0.15
A-5-5	1.84	3.75	0.05	0.07
A-2-5	1.94	3.60	0.04	0.10
A-1-5	2.12	3.73	0.04	0.16
A-5-15	1.51	3.37	0.04	0.23
A-5-10	1.70	3.56	0.04	0.20
A-5-2	1.87	3.75	0.04	0.09
A-5-1	1.94	3.78	0.03	0.10
B-5-5	1.67	2.75	0.06	0.24
C-5-5	1.49	2.26	0.05	0.22

Due to the effects of the mixture of "hot" Ar and Ar^+ with "cold" C_2H_2, the thermo-fluid-dynamic parameters, as per the Mach number at the inlet section, are different from those that one could expect from the flow in nozzles with different area ratio; the higher is the area ratio, the higher is the Mach number. In the present tests, Ma_i for nozzle A is higher than the ones for nozzles B and C and Ma_i for nozzle B is higher than the one for nozzle C. It looks that x_s does not change meaningfully by changing test parameters; the maximum fluctuation is 0.03 m. On the contrary, nozzle influences strongly both intensity and extension of the shock wave. In fact, Ma_{max} and Δx_s are about 3.75, 2.75, 2.26 and 0.07, 0.24, 0.22 m for nozzle A, B and C, respectively. The percentage
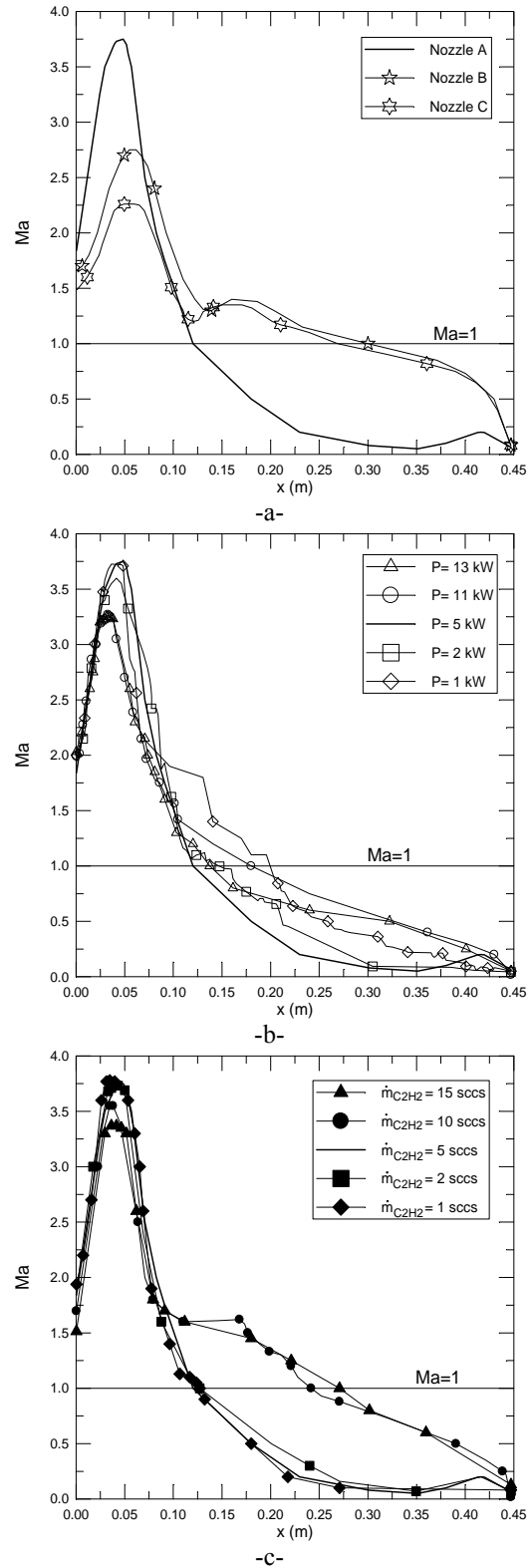

Fig. 8 Profiles of Mach number along the chamber axis by nozzle A, B and C (a), by different electrical power (b) and by different mass flow rate of C_2H_2 (c)

World Academy of Science, Engineering and Technology
International Journal of Aerospace and Mechanical Engineering
Vol:4, No:11, 2010

decrease of Ma_{max} for nozzle B and C, with respect to the one for nozzle A, are 27% and 40%, respectively. The percentage increase of Δx_s for nozzle B and C are 243% and 214%, respectively.

The effects of the electrical power and of the mass flow rate on the intensity of the shock wave look to be not very strong; in the power interval 1-13 kW, Ma_{max} ranges from 3.73 to 3.25; the percentage decrease is 13%. In the interval of mass flow rate 1-15 sccs, Ma_{max} ranges from 3.78 to 3.37; the percentage decrease is 11%. On the opposite, the influence of these parameters is pretty strong on the thickness of the shock wave. By increasing power, Δx_s decreases from 0.16 to 0.11 m; the percentage decrease is 31%. Increasing the mass flow rate, Δx_s ranges from 0.10 to 0.23 m; the percentage increase is 130%.

For the evaluation of the effects of test conditions on fluid-dynamic parameters, Fig. 9 and Fig. 10 report the profiles of temperature and velocity along the radius of the chamber at a station (x=0.2 m) along the chamber axis, located roughly mid-way between the inlet section (x=0) and the substrate (x=0.45 m), as functions of nozzle (a), electrical power (b) and mass flow rate of C_2H_2 (c), respectively.

Profiles of temperature and velocity roughly agree with the values at the inlet section (see Table II). The higher is temperature at the inlet of the chamber (or input to DS2V), the higher is temperature in the chamber. Furthermore, to satisfy the constancy of the mass flow rate, an opposite influence of density is produced on velocity. In fact, the higher is density, quantified by the number density (see Table II), the lower is velocity. All effects look to be pretty strong for both quantities. For example, considering as reference data the ones from test A-5-5, profiles of temperature and values at the chamber axis from the nozzles reproduce the values at the inlet (Fig. 9a); increasing power to 13 kW, temperature at the axis practically doubles, as well as, reducing $\dot{m}_{C2H2}$ to 1 sccs, temperature increases of a factor of about 1.5. As reported in Table II, using nozzles B and C, density practically behalves and velocity practically doubles (Fig. 10a). By increasing power, or temperature, density decreases, involving an increase of velocity. By a power of 13 kW, velocity at the axis practically triples. While, for $\dot{m}_{C2H2}$=1 sccs velocity at the axis increases of a factor of about 2.5.

Notwithstanding the deposition chamber in Eindhoven is not precisely simulated (as per: i) geometrical characteristics of the conducts of torch and nozzle, ii) pressure produced by the pump and therefore exit velocity V_E, iii) actually C2H2 is injected by an injection ring, located at 0.05 m from the inlet section), however some fluid-dynamic results look to be encouraging. From test A-5-5, as said before close to the experimental conditions: i) position of the shock wave, along the chamber axis, agrees perfectly with that measured by Benedickt [12] (x_s=0.05 m), ii) velocity, after the shock (at x=0.06 m), is 2640 m/s, velocity, measured by Engeln and reported by Benedikt [12], is 2000 m/s, iii) average pressure along the chamber axis is about 40.7 N/m², pressure measured
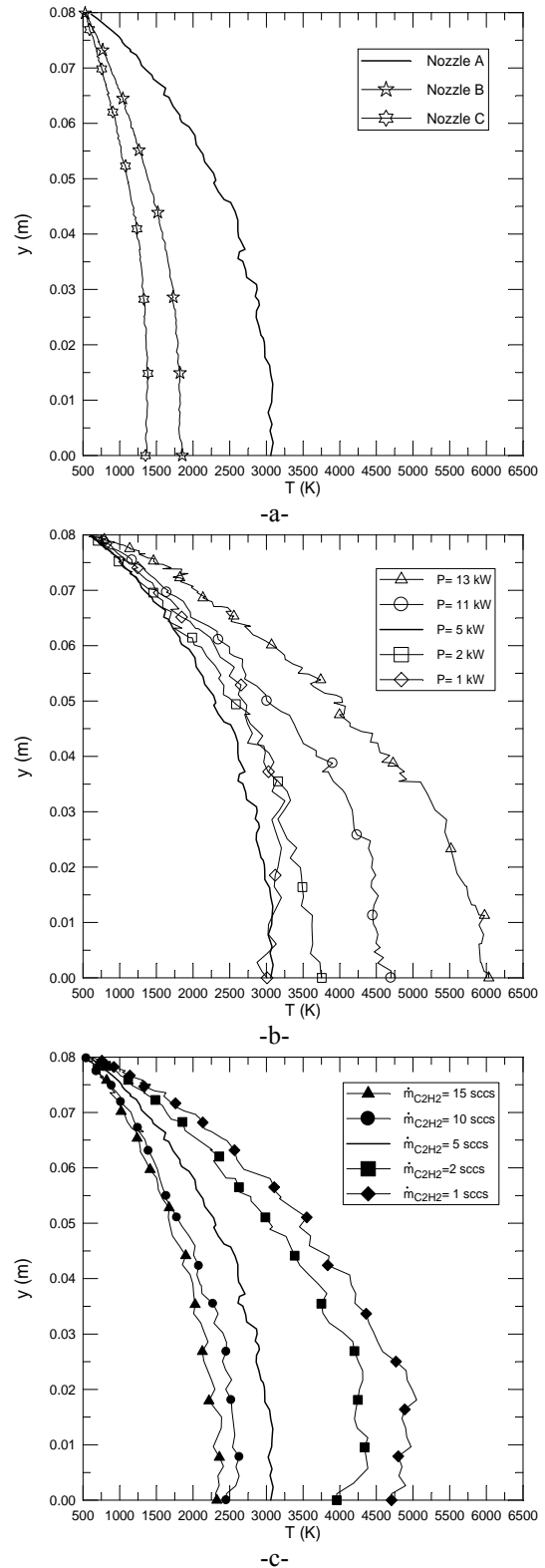

-a-

-b-

-c-

Fig. 9 Profiles of temperature along the radius of the chamber at x=0.2 m by nozzle A, B and C (a), by different electrical power (b) and by different mass flow rate of C_2H_2 (c)

World Academy of Science, Engineering and Technology
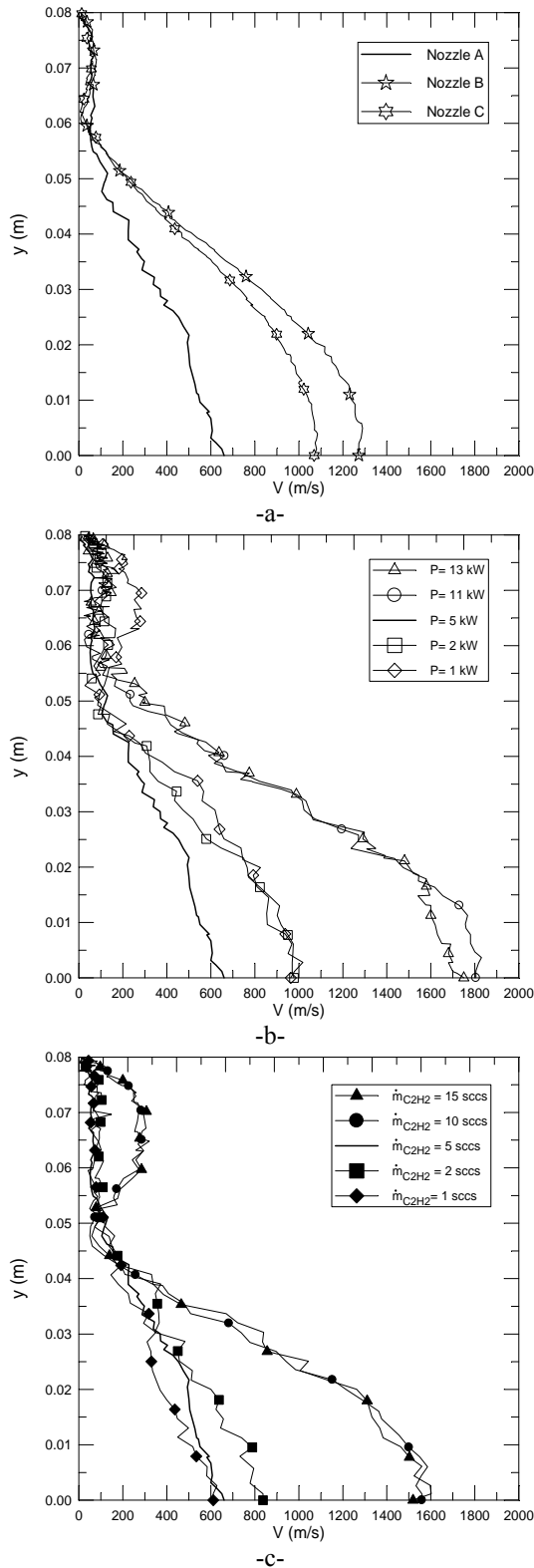International Journal of Aerospace and Mechanical Engineering
Vol:4, No:11, 2010

Fig. 10 Profiles of velocity along the radius of the chamber at x=0.2 m by nozzle A, B and C (a), by different electrical power (b) and by different mass flow rate of C_2H_2 (c)

in the deposition chamber is about 29 N/m^2 [12], [13].

D. Film

Fig. 11 shows, for test A-5-5, the 2-D maps in the chamber of the molar fractions of C_2 that, as already said, makes the film together with C, CH and C_2H. The influence of test conditions on the molar fractions of these chemical species is quantified by the average values on the chamber of each chemical species as well as of the sum of these molar fractions ($\overline{\alpha}_{tot}$); Table IV reports these values for all tests.
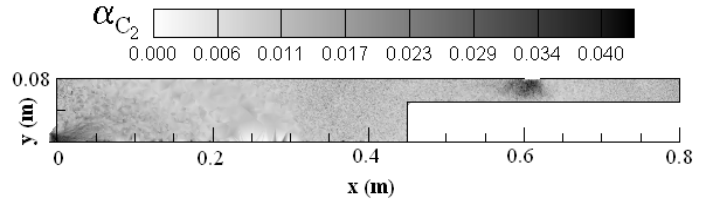

Fig. 11 2-D map of the molar fractions of C_2 in the deposition chamber: test A-5-5

TABLE IV
AVERAGE MOLAR FRACTION IN THE CHAMBER

Test	$\overline{\alpha}_C$	$\overline{\alpha}_{C_2}$	$\overline{\alpha}_{CH}$	$\overline{\alpha}_{C_2H}$	$\overline{\alpha}_{tot}$
A-13-5	0.1664	0.0319	0.0291	0.0005	0.2279
A-11-5	0.2241	0.0003	0.0003	0.0000	0.2247
A-5-5	0.2067	0.0050	0.0092	0.0001	0.2210
A-2-5	0.0275	0.0023	0.0033	0.0002	0.0333
A-1-5	0.0000	0.0000	0.0000	0.0000	0.0000
A-5-15	0.0012	0.0001	0.0001	0.0001	0.0014
A-5-10	0.0749	0.0086	0.0090	0.0003	0.0928
A-5-2	0.2029	0.0000	0.0000	0.0000	0.2029
A-5-1	0.1360	0.0000	0.0000	0.0000	0.1360
B-5-5	0.0000	0.0000	0.0000	0.0000	0.0000
C-5-5	0.0000	0.0000	0.0000	0.0000	0.0000

As seen before (Fig. 4), increasing power produces an increase of the molar fraction of Ar+, therefore an increase of reactivity of the mixture and finally an increase of the species making the film. It looks that using a power higher than 5 kW is not necessary because the total molar fraction does not changes significantly. On the other hand, using a power lower than 5 kW produces low molar fraction; $\overline{\alpha}_{tot}$ decreases of 85% in the range 13-5 kW. No chemical species useful for the film is produced by P=1 kW. The influence of the mass flow rate is not monotonic. In fact, increasing the mass flow rate does not produce an increase of $\overline{\alpha}_{tot}$; maximum molar fraction is met at $\dot{m}_{C2H2}$=5 sccs.

DS2V provides in output the number flux (N_f) of molecules impinged onto a surface and more specifically, for the interest of the present application, onto the substrate. This quantity can provide very preliminary information on the film thickness and uniformity of its distribution. Table V reports, for each test, the average value of the molecule flux ($\overline{N}_f$) with the related standard deviation (σ). In agreement with what reported by Mizuseki [21], these parameters can be considered as measures of the film thickness and its uniformity, respectively;

World Academy of Science, Engineering and Technology
International Journal of Aerospace and Mechanical Engineering
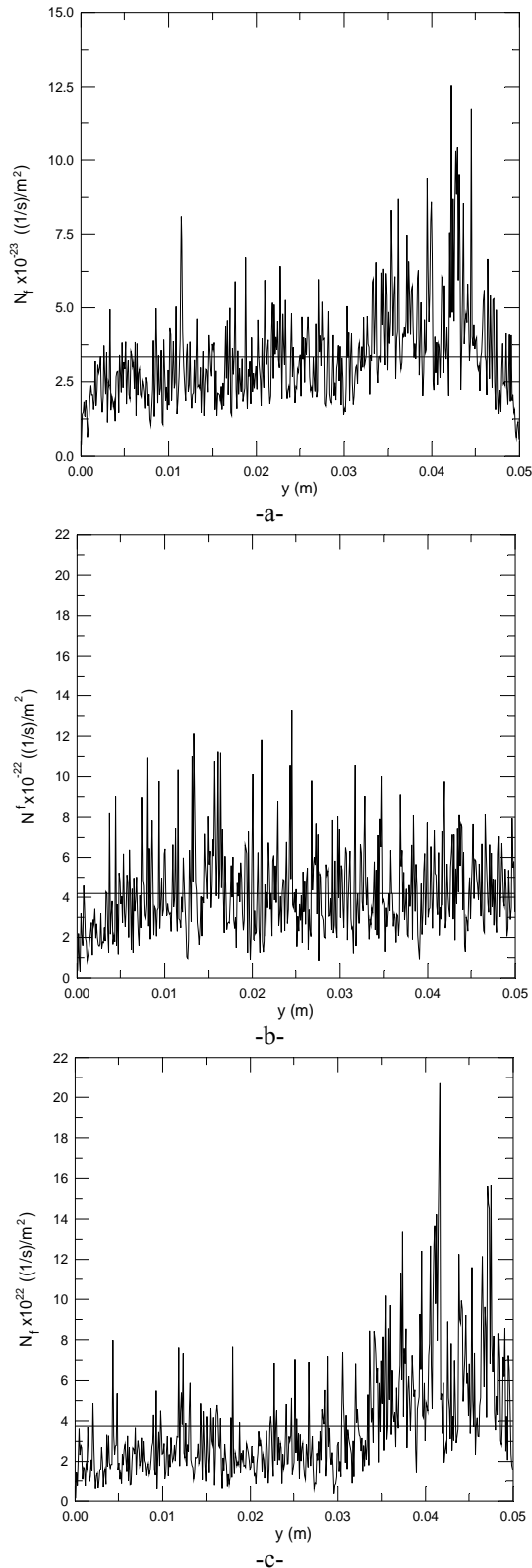Vol:4, No:11, 2010

-a-

-b-

Fig. 12 Profile of the molecule number flux on the substrate surface for test A-5-5 (a), A-13-5 (b) and A-5-10 (c); the straight line represents the average value

the higher is $\overline{N}_f$, the ticker is the film and the smaller is σ, the more uniform is the film. The average values of $\overline{N}_f$ for each chemical species are also reported. Fig. 12 reports the profiles of N_f on the substrate for test A-5-5 (a), for high power test A-13-5 (b) and for high mass flow rate test A-5-10 (c). As shown in Fig. 12 and also reported in Table V, the higher are the power and the mass flow rate, the thicker and the less uniform are the films.

TABLE V
NUMBER FLUX×10^{-22} (M^{-2}S^{-1}) AND STANDARD DEVIATION×10^{-22} (M^{-2}S^{-1}) OF MOLECULES IMPINGED ONTO THE SUBSTRATE

Test	$\overline{N}_f$	σ	$\overline{N}_{fC}$	$\overline{N}_{fC2}$	$\overline{N}_{fCH}$	$\overline{N}_{fC2H}$
A-13-5	4.18	2.17	1.05	1.06	1.05	1.03
A-11-5	1.00	0.23	1.00	0.00	0.00	0.00
A-5-5	3.34	1.69	0.83	0.84	0.83	0.85
A-2-5	1.63	1.60	0.40	0.40	0.40	0.43
A-1-5	0.00	0.00	0.00	0.00	0.00	0.00
A-5-15	0.94	4.77	0.49	0.00	0.45	0.00
A-5-10	3.79	3.00	0.95	0.96	0.96	0.93
A-5-2	0.97	0.41	0.97	0.00	0.00	0.00
A-5-1	0.51	0.24	0.51	0.00	0.00	0.00
B-5-5	0.71	2.97	0.18	0.17	0.18	0.17
C-5-5	0.64	6.18	0.14	0.18	0.18	0.14

As shown in Table V, a power of 1 kW is too low for producing film. Furthermore, the lower is the mass flow rate, the smaller is the number flux therefore the more thin is the thickness of the film and the smaller is its uniformity.

It looks that the larger is the nozzle exit section, the smaller is the film thickness but the higher is the film uniformity. Furthermore the contribution of each chemical species to form the film is practically the same. Even with the limitations in the present simulations, using nozzle A, $\dot{m}_{C2H2} = 5$ sccs and P=5 kW, makes the best compromise between the thickness and the distribution uniformity of the film.

VII. CONCLUSIONS AND FURTHER DEVELOPMENTS

A computing procedure has been proposed as a possible tool for the evaluation of the effects of operating parameters on fluidics of a typical ETP deposition chamber. For this purpose a chamber similar in shape, dimensions and operating parameters to that at the University of Eindowen has been simulated. The procedure relies on two codes working in tandem; the output from the first one is the input to the second one. The first code solves a quasi-one-dimensional, continuum flow field in the torch and in the nozzle, the second code solves the flow field in the chamber by the DSMC method. The DSMC code is the commercial DS2V. Both codes are able to consider 21 chemical species and implement 24 chemical reactions, typical of a mixture of Argon plasma and Acetylene. A post run rarefaction analysis verified that the flow field in the chamber is rarefied enough for a proper application of the DSMC method.

A sensitivity analysis of the thermo-fluid-dynamic parameters has been also carried out. The effects of the electrical power, supplied to the torch, of the precursor mass

World Academy of Science, Engineering and Technology
International Journal of Aerospace and Mechanical Engineering
Vol:4, No:11, 2010

flow rate and of the nozzle have been evaluated and quantified, such as position, intensity and extension of the shock wave. More specifically, the effects of electrical power as well as of mass flow rate look to be not very strong on intensity of the shock wave. On the opposite, this influence is pretty strong on thickness of the shock wave.

Besides the sensitivity analysis on some fluid-dynamic parameters, the effects of the above mentioned test parameters have been evaluated on the number flux of molecules impinged onto the substrate. This quantity can provide preliminary information on the film thickness and uniformity of its distribution. The present analysis verified that increasing electrical power and precursor mass flow rate increases the average molecule number flux, therefore the film thickness and also the related standard deviation; making less uniform the film.

Evaluating the cross-effects of electrical power and mass flow rate and the effects of wall surface reactions has been already scheduled for completing the present sensitivity analysis.

REFERENCES

[1] M.C.M. van de Sanden, R.J. Severens, J.W.A.M. Gielen, R.M.J. Paffen and D.C. Schram, "Deposition of a–Si:H and a-C:H using an expanding thermal arc plasma", Plasma Sources Sci. Technol., vol. 5, pp. 268-274 , 1996.
[2] M.C.M. van de Sanden, J.M. Regt and D.C. Schram, "The behaviour of heavy particles in the expanding plasma jet in argon", Plasma Sources Sci.Technol.,vol.3, pp. 501-510 ,1994.
[3] K.J. Kuijlaars, "Detailed modelling of chemistry and transport phenomena in CVD reactors", Ph.D. Thesis, TUDelft, 1996.
[4] E. Neyts, "Mathematical simulation of the deposition of diamond-like carbon (DLC) films", Ph.D. Thesis, University of Antwerpen, 2006.
[5] S,E. Selezneva, M.I. Boulos, M. C. M. van de Sanden, R. Engeln, D.C. Schram, "Stationary supersonic plasma expansion: continuum fluid mechanics versus direct simulation Monte Carlo method", J. Phys. D, vol. 35, pp. 1362-1372, 2002.
[6] G. Abbate, "Multi-scale modelling of gas flows with continuum-rarefied transitions", Ph.D. Thesis, TUDelft, 2009.
[7]   G. Abbate, C.R. Kleijn, B.J. Thijsse, R. Engeln, M.C.M. van de Sanden and D.C. Schram, "Influence of rarefaction on the flow dynamics of a stationary supersonic hot-gas expansion", Physical Review E, vol. 77 036703, 2008.
[8] G.A. Bird, "The DS2V program user's guide, (Version 4.3)" (included in the program), G.A.B. Consulting Pty Ltd, Sydney, 2006.
[9] G. Zuppardi, F. Romano, "Direct Simulation Monte Carlo Method in Industrial Applications" in Direct Simulation Monte Carlo, Theory, Methods & Applications, (DSMC09) Workshop, Santa Fe, 2009.
[10] Yu.A. Mankelevich, N.V. Suetin, M.N.R. Ashfold, W.E. Boxford, A.J. Orr-Ewing, J.A. Smith and J.B. Wills, "Chemical kinetics in carbon deposition d.c.-arc jet CVD reactors", Diamond and Related Materials, vol. 12, pp. 383-390, 2003.
[11] D:A: Ariskin, I.V. Schweighert, A.L. Alexandrov, A. Bogaert and F.M. Peeters, "Modeling of chemical processes in the low pressure capacitive radio frequency discharges in a mixture of Ar/C_2H_2", Journal of Applied Physics , vol. 105, 063305, 2009.
[12] J. Benedikt, D. C. Schram and M. C. M. van de Sanden, "Detailed TIMS study of Ar/C_2H_2 expanding thermal plasma: identification of a-C:H film growth precursors", J. Phys. Chem. A, vol. 109, 10153, 2005.
[13] J. Benedikt, S. Agarwal, D. Eijkman, W. Vandamme, M. Creatore and M. C. M. van de Sanden, "Thereshold ionization mass spectrometry of reactive species in remote Ar/C2H2 expanding thermal plasma", J. Vac. Sci. Technol. A, vol. 23, pp. 1400-1411, 2005.
[14] G.A. Bird, "Molecular gas dynamics and Direct Simulation Monte Carlo", Oxford, Clarendon, 1998.
[15] C. Shen , "Rarefied gas dynamic: fundamentals, simulations and micro flows", Berlin, Springer-Verlag, 2005.
[16] G.A. Bird, "Sophisticated versus simple DSMC", in 2006 25th International Symposium on Rarefied Gas Dynamics, Saint Petersburg, pp. 349-354.
[17] G.A. Bird, "Sophisticated DSMC", notes from a short course held at the DSMC07 Conference, Santa Fe, 2007.
[18] G. Zuppardi, A. Esposito, "Blowdown arc facility for low-density hypersonic wind-tunnel testing", Journal of Spacecraft and Rokets, vol. 38, pp. 946-948, Nov.-Dec 2001.
[19] G.P. Russo, G. Zuppardi, A. Esposito, "Computed versus measured force coefficients on a cone in a small arc facility", Journal of Aerospace Engineering, vol. 222 Part G, pp.403-409, May 2008.
[20] J. D. Cobine, "Gaseous conductors theory and engineering applications", New York, Dover   Publication, 1958.
[21] H. Mizuseki, K. Hongo, Y. Kawazoe, L.T. Wille, "Multiscale simulation of cluster growth and deposition processes by hybrid model based on direct simulation Monte Carlo method", Computational Materials Science, vol. 24, pp. 88-92, 2002.